

RHEOLOGICAL BEHAVIOR OF SS316L GAS ATOMIZED POWDER IN BIMODAL PARTICLE SIZE DISTRIBUTION IN A COMPOSITE BINDER SYSTEM

K. R. Jamaludin^a, N. Muhamad^b, S. Y. M. Amin^c, M. N. Ab. Rahman^b and Murtadhahadi^d

^aDepartment of Mechanical Engineering, College of Science and Technology, Universiti Teknologi Malaysia City Campus, 54100 Kuala Lumpur, Malaysia

^bPrecision Process Research Group, Dept. of Mechanical and Materials Engineering, Faculty of Engineering Universiti Kebangsaan Malaysia, 43600 Bangi, Selangor, Malaysia

^cDepartment of Mechanical and Manufacturing, Universiti Tun Hussein Onn Malaysia 86400 Batu Pahat, Johor, Malaysia

^dDepartment of Mechanical Engineering, Lhokseumawe State Polytechnic, Aceh, Indonesia
Email: khairur@citycampus.utm.my

ABSTRACT

Rheological properties of the monomodal and bimodal MIM feedstock are presented in this paper. Coarse and fine SS316L gas atomized powders are mixed with PEG and PMMA to form a homogenous paste, which is termed as feedstock. The surface active agent used here is stearic acid. The bimodal powders are blended from 30 to 70 % of the coarse powder distribution. Results show that monomodal feedstock exhibits a higher viscosity over the bimodal feedstock at low shear rate. Binder separation is also likely to occur in the monomodal feedstock prepared with coarse powder especially at a high injection temperature. Furthermore, bimodal feedstock is less viscous than the monomodal feedstock but the particle size distribution has shown its influence on viscosity. The flow behavior index decreases when the temperature increases. The investigation also shows that the feedstock flow sensitivity depends on the fine powder distributions in the feedstock. Since all the feedstock demonstrates a good pseudo plastic behavior, it therefore is suitable to be injection molded.

Keywords: Particle size distribution, Rheology, MIM feedstock, flow sensitivity, bimodal.

1. INTRODUCTION

Metal injection molding (MIM) is a near-net shaped processing technique that permits manufacturing of complex components. Fabrication starts by compounding a thermoplastic binder and powder metal mixture, referred to as feedstock, followed by injection molding, binder removal and sintering (Suri *et al.*, 2003).

This advanced manufacturing process is a modification of the common injection molding process for plastics where a significant volume fraction of plastic is replaced

by a fine metal powder with a plastic binder to form a paste feedstock and injection molding, a “green” part using the specific feedstock on a conventional thermoplastic molding equipment. The major advantages from this manufacturing process include high product density, a more intricate shape, higher mechanical properties, and a better surface finish over the traditional powder metallurgy products. Moreover, an inherent advantage of MIM is that the molding parts are hard enough to meet any needs for secondary machining (Huang *et al.*, 2003).

The requirement for small particle dimensions has led to some concerns regarding the potential cost of the process, making MIM a relatively expensive route for the production of larger components. Therefore, a primary motivation for adding coarser particles to fine powders is to lower the costs. However, there are some disadvantages of the method that may lead to the non-homogeneity in the sintered structure. Thus, avoidance of component defects requires a quantitative understanding of the effects of process parameters on the rheological behavior of MIM feedstock. This is an important topic in MIM where the desire is to minimize the binder content and the sintering shrinkage using bimodal mixture (German and Bulger, 1992a). Besides, broad particle size distributions or bimodal distributions are desirable to maximize the solid content, since the small particles fill interstitial space and release the binder to lubricate particle flow (German and Bose, 1997). In addition, mixtures of powders with differing sizes give improved packing densities over that available from either powder itself (German and Bulger 1992a, 1992b; German, 1992).

The rheological investigation described below employed bimodal powder blends with polymethyl methacrylate (PMMA), polyethylene glycol (PEG) and stearic acid as a binder system. Capillary rheometry was employed to analyze the flow behavior of the feedstock. The

information obtained from the experiment provides measurement of feedstock viscosity at a variable shear rate to evaluate the feedstock stability and prediction of the separation phenomena, analysis of the viscosity and shear rate to obtain the flow behavior index, activation energy and general rheological index that indicate the stability of the feedstock as well as its suitability to the process. The bimodal particle feedstock rheological parameters are compared with the monomodal to show the significance of the injection parameters.

2. METHODOLOGY

In this work, commercial gas atomized stainless steel powder 316L with particle sizes of 19.521 μm and 11.225 μm are mixed with PMMA, PEG and stearic acid. The rheological characteristic of the feedstock was investigated using a Shimadzu 500-D capillary rheometer. In a prior investigation, stainless steel powder was mixed with binders in a Sigma type blade mixer for 95 minutes at 70 °C. Four compositions of feedstock consisting of different particle distributions were prepared for the investigation as shown in Table 1.

Table 1 Feedstock classification and the powder loading remains at 64 % vol.

| Feedstock Abbreviation | Description |
|------------------------|------------------------------------|
| 31_64 | Monomodal: coarse powder |
| 16_64 | Monomodal: fine powder |
| A1_64 | Bimodal: 70% mass of coarse powder |
| B1_64 | Bimodal: 30% mass of fine powder |

3. RESULTS AND DISCUSSION

3.1 Viscosity dependence to shear rate

Figures 1, 2 and 3 show the correlation of viscosity and shear rate at injection temperatures of 120 °C, 130 °C, and 140 °C. These temperatures were selected based on Omar's (1999) work, which studies the injection parameters of the MIM feedstock prepared with the same materials as those presented in this paper. The bimodal feedstock, A1_64 as shown in Figure 1 exhibits the highest viscosity at shear rate nearly 4000 s^{-1} while B1_64 is at the lowest viscosity when the shear rate is in between 6000 s^{-1} to 8000 s^{-1} . Furthermore, as shown in Figure 1 the A1_64 is unexpectedly is demonstrated the lowest viscosity at shear rate above 10,000 s^{-1} . This is an evidence of the occurrence of powder-binder separation where, the viscosity is unexpectedly low at a very high shear rate. Another indication of powder-binder

separation is the viscosity is suddenly plummeting before it jumped back at higher shear rate.

Additionally, when the temperature was increased to 130 °C (Figure 2) the A1_64 melt viscosity is reduced. Furthermore, the feedstock became inhomogeneous due to powder and binder separation (Heaney and Zauner, 2003). Thus, Maetzig *et al.* (2002) suggested maintaining the injection molding at relatively low flow rate in order to prevent separation of powder and binder. When the injection temperature was increased to 130 °C, the bimodal feedstock, B1_64 exhibited a higher viscosity at a shear rate less than 4000 s^{-1} as compared to the monomodal feedstocks. Moreover, Figure 2 also shows that A1_64 is less viscous than the B1_64. This is due to the higher inter-particle friction between B1_64 powder particle and thus it minimizing the shear rate and increasing the melt viscosity.

Moreover, when the temperature was increased to the maximum (Figure 3), the monomodal feedstock, 31_64 became more viscous than the 16_64. Figure 3 shows that the shear rate of the fine powder (16_64) is higher than the coarse powder (31_64). This phenomenon occurred possibly due to the 31_64 coarse powder is left behind the binder when 31_64 is extruded through the capillary at 140 °C. Fine powders prevent the feedstock from powder-binder separation during injection molding, as this effect is more likely to be introduced through large particles, especially when a low viscosity binder and metal powders of high density are used (Rath *et al.*, 2005). Furthermore, both bimodal particle sized distribution feedstock, demonstrates an equivalent shear rate at 140 °C compared to what has been shown in Figure 1 and Figure 2. Conversely, Resende *et al.* (2001) discovers that using carbonyl iron powder that particle distribution does not affect viscosity for powder fraction of 60 % volume as the monomodal and bimodal distributions present the same viscosity because the shear rate was varied. As the powder fraction was increased from 60 % to 65 % volume in a bimodal distribution, the viscosity was less affected than when the powder fraction was increased from 55 % to 60 % volume in a monomodal distribution. Finally, he concludes that the bimodal distribution for carbonyl iron powder is to be recommended only for very high powder loading. Particle size ratio in the bimodal powder distribution system has its significance. A large particle size ratio can also provide higher packing density, better stability in debinding, good moldability, and lower shrinkage in sintering. However, there are a number of problems associated with such blends and these include larger clearances needed between the screw and barrel in the molding machine, and the potential for non-homogeneity in the sintered structure, which can adversely affect the part's physical and mechanical properties (Dihoru *et al.*, 2000).

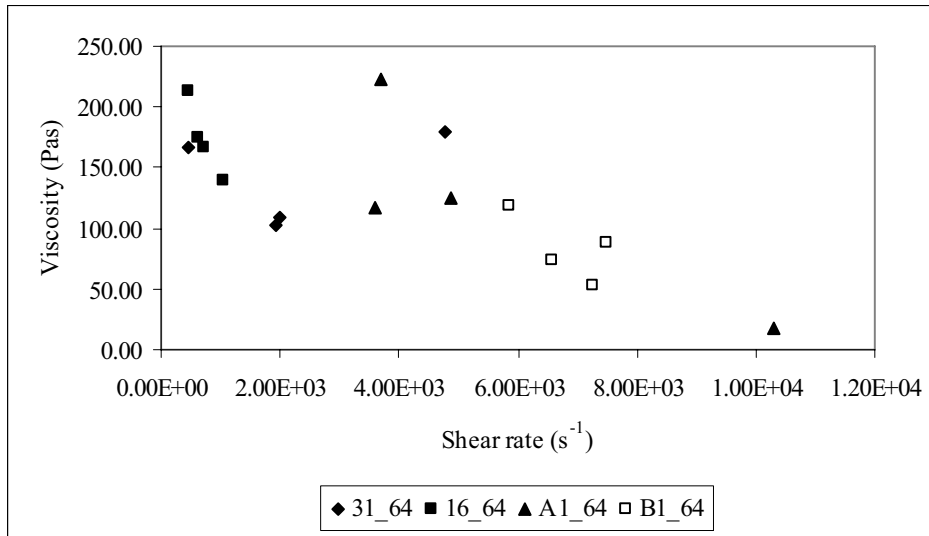


Figure 1 Correlation of viscosity and shear rate at 120 °C

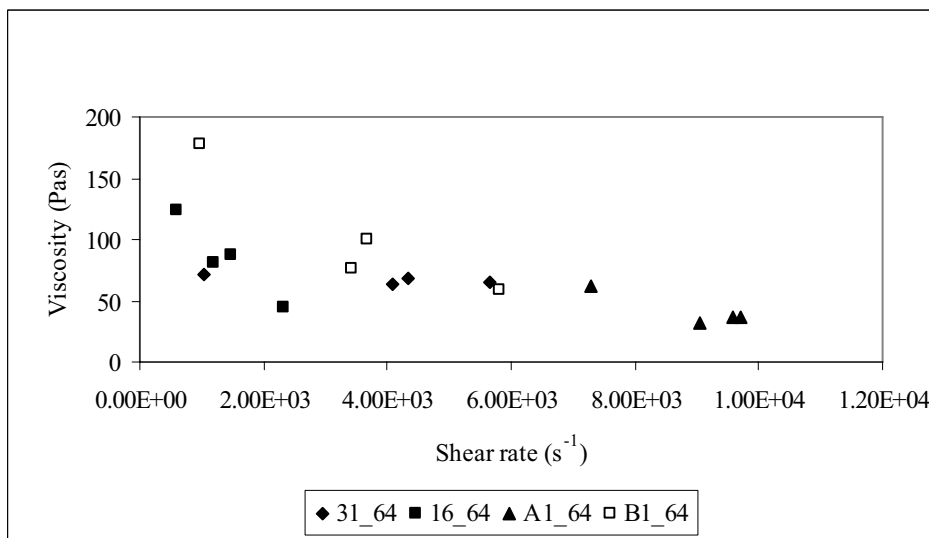


Figure 2 Correlation of viscosity and shear rate at 130 °C

Figure 1 indicates that the coarse powder feedstock (31_64) is less viscous than the fine powder feedstock (16_64). On the other hand in Figure 2, the viscosity of 31_64 is also lesser than the 16_64 at shear rate above 2000 s⁻¹, but the viscosity of the 16_64 is plummeting when at shear rate above 2000 s⁻¹.

Likewise when the melt temperature is increased to 140°C (Figure 3), 16_64 is found to be less viscous than the 31_64 at shear rate above 4000 s⁻¹. The 31_64 viscosity is lesser than the 16_64 at temperature 120 °C and 130 °C, this indicates that the coarse particles in a

system diffuse to a lesser extent than the fine powder and less energy is dissipated in the flow. Consequently, by adding coarse powder to the fine powder, a feedstock with lower relative viscosity at the same solid loading content can be obtained (Dihoru *et al.*, 2000).

A binder separation phenomenon is likely to occur when the viscosity is increased at high shear rate or when the viscosity is suddenly plummet before it jumped at higher shear rate. Modeling the binder separation phenomenon as flow through porous medium enables identification of the parameters influencing the separation that occurs

during the tests. The following equations (Kozeny-Carman and the Blake Kozeny equation respectively) describe the permeability constant of a porous medium, k

$$k = \frac{\varphi^3}{5S^2(1-\varphi)^2} \quad (1a)$$

$$k = \frac{D^2\varphi^3}{150(1-\varphi)^2} \quad (1b)$$

where φ is medium porosity; S is specific pore surface (pore surface exposed to the fluid per unit volume of a porous material); D is particle diameter.

These two relations show that the permeability constant is low when the particle size is small and the pore surface area is large. Binder separation is less likely to occur when the flow through the porous medium is low, which is equivalent to a lower permeability value.

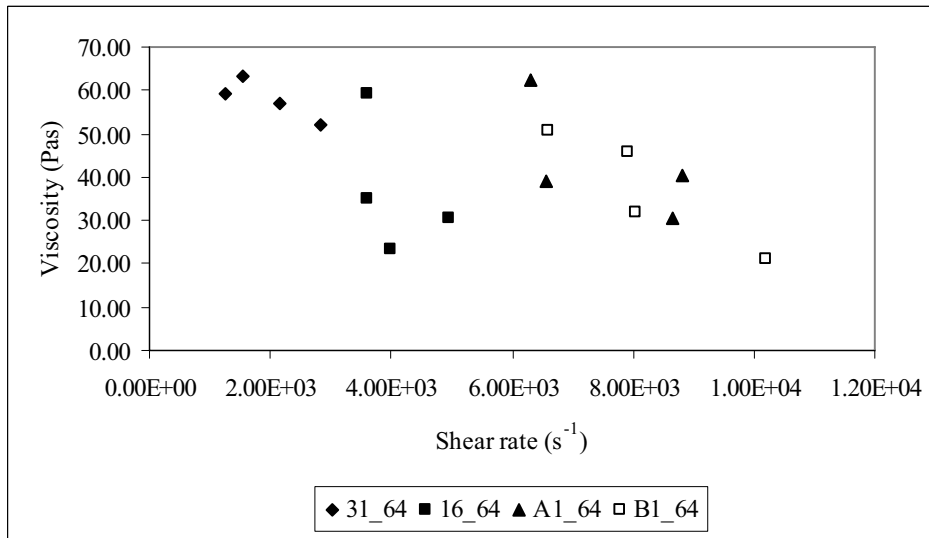


Figure 3 Correlation of viscosity and shear rate at 140 °C

3.2 Temperature influence

Figures 4 and 5 show the feedstock viscosity dependence on temperature. The error bars indicate the maximum and minimum viscosities. As shown in Figure 4, A1_64 has a broad viscosity range from temperatures of 120 and 125 °C, when it was extruded at 29 bars from the rheology test barrel. Besides, Figure 5, B1_64 shows a wide viscosity range at 130 °C when pressures at bars 29 and 59 were applied. As shown in Figure 4, viscosity decreases when the extrusion pressure and the test temperature is increased, regardless, in Figure 5 the viscosity fluctuates with the increase of temperature. This is possibly due to the occurrence of binder separation as the feedstock in Figure 5 has broader coarse powder distribution as compared to A1_64.

3.3 Feedstock pseudo plasticity

A regression line of the scatter plot shown in Figures 1, 2 and 3 can be rewritten as

$$\eta = K \dot{\gamma}^{n-1} \quad (2)$$

where η is the viscosity at shear rate of $\dot{\gamma}$, K is a constant and, n is a flow behavior index. Equation (2) has been widely used to correlate the data of viscosity to shear rate for pseudo plastic and dilatant fluids, which is known as the power-law equation. The flow behavior index, n of the power-law index indicates the shear sensitivity. Smaller n of feedstock indicates higher shear sensitivity and more pseudo plasticity of the feedstocks. Some molding defects such as jetting are associated with small n , i.e., higher shear sensitivity (Yang *et al.*, 2002). During the injection molding process, pseudo plastic behavior is desirable and, therefore, a decrease in viscosity with an increase in the shear rate is suitable. This dependent behavior of the viscosity against the shear rate is especially important when producing complex and delicate parts, which are vital products in the Metal Injection Molding (MIM) industry (Agote *et al.*, 2001). In Table 2, a comparison of the feedstocks is shown.

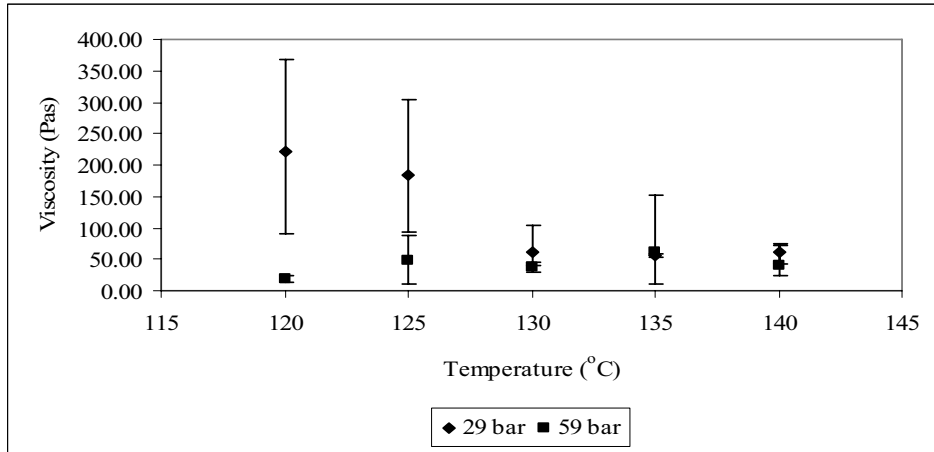


Figure 4 Temperature influence to the viscosity for A1_64

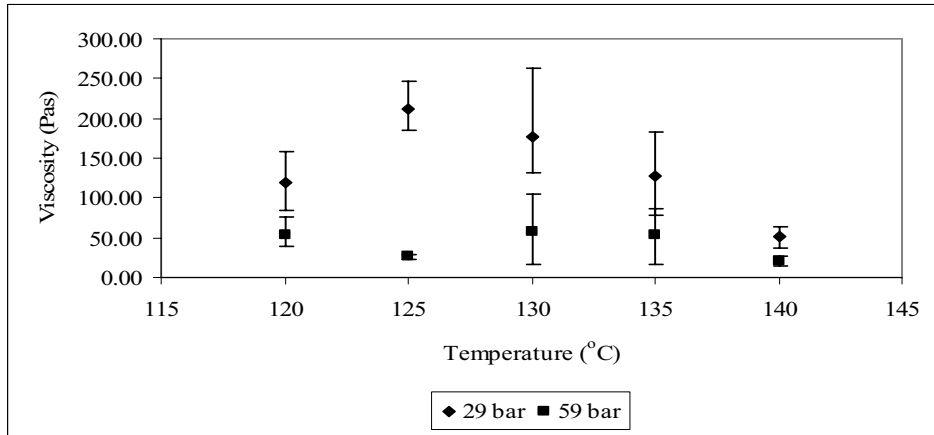


Figure 5 Temperature influence on the viscosity for B1_64

Generally, the feedstocks in Table 2 demonstrate pseudo plasticity as the index is smaller than one, thus it indicates shear thinning occurs in the feedstock when applied to a shear stress. The flow behavior index of 16_64 is smaller than 31_64. This indicates that at shear rate 16_64 the viscosity of the feedstock changes more quickly. The coarse powder is likely to become dilatant at a low temperature, as the flow behavior index for 31_64 seems inversely proportional to the temperature and is expected that the value becomes higher than unity. Furthermore, B1_64 exhibits high sensitivity than A1_64. However, the sensitivity of B1_64 reduces with the increase of temperature. The sensitivity of A1_64 is high due to the high fine powder composition in the bimodal system as compared to B1_64, which shows inconsistency of the flow behavior index when the temperature increases. In addition, the controllability of viscosity within an injection molding barrel by controlling the temperature of barrel, nozzle and mold, the temperature dependence of viscosity may have an effect on the response of the material to the sudden non-

uniform cooling within a cavity. For example, during the molding stage, the feedstock is forced into the mold where it immediately begins to cool. If the cooling is accompanied by a rapid increase in the viscosity, the result may be incomplete filling of the mold and induces cracking or porosity in the molded parts. Therefore, low temperature dependence is desired to minimize problems arising from fluctuating molding temperatures, thereby minimizing stress concentration, cracks and shape distortions (German and Bose, 1997; Hausnerova *et al.*, 2006). The value of flow activation energy, E as shown in Table 2 represents the influence of temperature on the viscosity of the feedstocks, is an important parameter for injection molding. The relationship of those properties in Table 2 is as shown in the equation below. The apparent viscosity is,

$$\eta = \eta_0 \exp\left(\frac{E}{RT}\right) \quad (3)$$

where R is the gas constant, T the temperature and η_0 the reference viscosity.

Taking nature logarithm at both sides, equation (4) is obtained

$$\ln \eta = \ln \eta_0 + \left(\frac{E}{R} \right) \frac{1}{T} \quad (4)$$

With a shear rate of 1000 s^{-1} , which falls in the normal range of shear rates for injection molding of MIM feedstocks, by plotting $\ln \eta$ against the reciprocal

temperature, the activation energies, E of viscous flow can be calculated and as given in Table 2. The activation energies and the viscosities at shear rate 1000 s^{-1} in Table 2 can cast some lights on the nature of the feedstocks.

The monomodal feedstock, 16_64 has low activation energy than 31_64 while the activation energy of the bimodal feedstock, A1_64 is lower than the B1_64. Nevertheless, the bimodal feedstock has low activation energies compared to the monomodal feedstock. Thus, it indicates that the bimodal feedstock is less sensitive to any temperature fluctuation during the injection molding process.

Table 2 Rheological properties of the feedstock

| Feedstock | Temp | Flow behavior index, n | Activation Energy, E | Apparent Viscosity, η | Moldability index, α_{STV} |
|-----------|------|------------------------|----------------------|----------------------------|-----------------------------------|
| 31_64 | 120 | 0.98 | 49.33 | 137.06 | 24.60 |
| | 130 | 0.95 | 49.33 | 71.62 | 117.68 |
| | 140 | 0.81 | 49.33 | 64.67 | 487.40 |
| 16_64 | 120 | 0.49 | 79.54 | 141.77 | 376.03 |
| | 130 | 0.23 | 79.54 | 94.44 | 852.24 |
| | 140 | -0.22 | 79.54 | 35.76 | 3571.93 |
| A1_64 | 120 | -1.12 | 24.43 | 2544.20 | 284.15 |
| | 130 | -1.00 | 24.43 | 2924.30 | 233.23 |
| | 140 | -0.16 | 24.43 | 323.89 | 1222.24 |
| B1_64 | 120 | -0.95 | 36.54 | 2850.56 | 155.66 |
| | 130 | 0.41 | 36.54 | 177.69 | 755.55 |
| | 140 | -1.06 | 36.54 | 2735.65 | 171.35 |

This feedstock can therefore be injection molded in a relatively wide temperature range. High activation energy of feedstock 31_64 indicates a drastic viscosity increase upon cooling, and thus feedstock 31_64 requires a more accurate temperature control during injection molding. Otherwise, mold temperature distribution will cause non-uniform flow, which induces internal stresses.

In order to establish a general molding index, the model Weir proposes for polymers to be used including the main parameters as regards to flow (Agote *et al.*, 2001).

$$\alpha_{STV} = \frac{1}{\eta_0} \frac{\left| \frac{\partial \log \eta}{\partial \log \dot{\gamma}} \right|}{\eta_0 \frac{\partial \log \eta}{\partial 1/T}} \quad (5)$$

where, η , is the viscosity η_0 is a reference viscosity T is the temperature $\dot{\gamma}$ is the shear rate and α_{STV} is the rheological index or moldability index (Li *et al.*, 1999). Simplifying the equation:

$$\alpha_{STV} = \frac{1}{\eta_0} \frac{|n-1|}{E/R} \quad (6)$$

The higher the value of α_{STV} , the better the rheological properties. In Table 2, 16_64 has better rheological properties at 140 °C while 31_64 has poor rheological property at 120 °C. In general, the rheological properties are proportional to the temperatures.

4. CONCLUSIONS

The rheological behavior of monomodal and bimodal stainless steel MIM feedstock have been investigated in terms of injection temperature (120-140 °C) and particle size distributions, over a wide range of shear rate. All feedstocks are possible to be injection molded as the flow behavior index indicates pseudo plastic behavior. The bimodal particle distribution enables to increase the shear rate and thus reduces the feedstock viscosity. B1_64 is less viscous as compared to A1_64 at 120 °C and 140 °C, however is vice versa at 130 °C. Further investigation is required to investigate why A1_64 is less viscous than the B1_64 at 130 °C. In addition, the B1_64 particle distribution is organized according to the Furnas model, which describes the ideal particle packing behavior of a binary powder system (Zheng et al., 1995). Furnas model suggests that the volume of fine particles is between 30 to 50 %. The bimodal feedstock also exhibits better pseudo plasticity as compared to the monomodal feedstock. Furthermore, the sensitivity of the viscosity to the temperature is also small thus; the bimodal feedstock is stable over a wide range of temperature.

REFERENCES

- Agote, I., Odriozola, A., Gutierrez, M., Santamaria, A., Quintanilla, J., Coupelle, P., and Soares, J., 2001. Rheological study of waste porcelain feedstocks for injection moulding. *Journal of the European Ceramic Society*, Volume 21, pp. 2843-2853.
- Dihoru, L. V., Smith, L. N., and German, R. M., 2000. Experimental analysis and neural network modeling of the rheological behavior of powder injection molding feedstocks formed with bimodal powder mixtures. *Powder Metallurgy*, Volume 43, No. 1, pp. 31-36.
- German, R.M., 1992. Prediction of sintered density for bimodal powder mixtures. *Metallurgical Transactions A*, Volume 23A, pp. 1455-1465.
- German, R.M., and Bose, A., 1997. *Injection Molding of Metal and Ceramic*, Metal Powder Industries Federation, Princeton, N.J.
- German, R.M., and Bulger, M., 1992a. A model for Densification by Sintering of Bimodal Particle Size Distributions. *International Journal of Powder Metallurgy*, Volume 28, No. 3, pp. 301-311.
- German, R.M., and Bulger, M., 1992b. The effects of bimodal particle size distribution on sintering of powder injection molded compacts. *Solid State Phenomena*, Volume 25 & 26, pp. 55-62.
- Hausnerova, B., Sedlacek, T., Slezak, R., and Saha, P., 2006. Pressure-dependent viscosity of powder injection moulding compounds. *Rheological Acta*, Volume 45, pp. 290-296.
- Heaney, D. F. and Zauner, R., 2003. Variability of feedstock and its effect on component dimensional variability. *Advances in Powder Metallurgy & Particulate Materials*, Volume 8, pp. 30-44.
- Huang, B., Liang, S., Qu, X., 2003. The rheology of metal injection molding. *Journal of Materials Processing Technology*, Volume 137, pp. 132-137.
- Li Y., H. Baiyun, and Xuanhui Q., 1999. Improvement of rheological and shape retention properties of wax-based MIM binder by multi-polymer components. *Transactions of Nonferrous Metals Society of China*, Volume 9, No. 1, pp. 22-29.
- Maetzig, M., Walcher, H., 2002. Strategies for injection moulding metals and ceramics. *Advances in Powder Metallurgy & Particulate Materials*, Volume 10, pp. 33-42.
- Omar, M.A., 1999. *Injection Molding of 316L Stainless steel and NiCrSiB alloy powder using a PEG/PMMA binder*. PhD Thesis, University of Sheffield, U.K.
- Rath, S., Merz, L., Plewa, K., Ruprecht, R. and Hausselt, J., 2005. Metal feedstocks for insolated micro parts made by PIM. *Advances in Powder Metallurgy & Particulate Materials*, Volume 4, pp. 84-92.
- Resende, L. M., Klein, A. N., and Prata, A. T., 2001. Rheological properties of granulometric mixtures for Powder Injection Molding. *Key Engineering Materials*, Volume 189-191, pp. 598-603.
- Suri, P., Atre, S.V., German, R.M., Souza, J.P., 2003. Effect of mixing on the rheology and particle characteristics of tungsten-based powder injection molding feedstock. *Materials Science and Engineering*, Volume A356, pp. 337-344.
- Yang, W. W., Yang, K. Y., and Hon, M. H., 2002. Effects of PEG molecular weights on rheological behavior of alumina injection molding feedstocks. *Materials Chemistry and Physics*, Volume 78, pp. 416-424.
- Zheng, J., Carlson, W. B., and Reed, J. S., 1995. The packing density of binary powder mixtures. *Journal of the European Ceramic Society*, Volume 15, pp. 479-483.